Applied Radiation and Isotopes 118 (2016) 281–289

Contents lists available at ScienceDirect

Applied Radiation and Isotopes

journal homepage: www.elsevier.com/locate/apradiso

Deuteron induced Tb-155 production, a theranostic isotope for SPECT imaging and auger therapy

C. Duchemin[a,*], A. Guertin[a], F. Haddad[a,b], N. Michel[a,b], V. Métivier[a]

[a] SUBATECH, Ecole des Mines de Nantes, Université de Nantes, CNRS/IN2P3, Nantes, France
[b] GIP Arronax, 1 rue Aronnax, 44817 Saint-Herblain, France

ARTICLE INFO

Keywords:
Terbium-155
Gadolinium target
Deuteron beam
Stacked-foil technique
TALYS 1.6

ABSTRACT

Several terbium isotopes are suited for diagnosis or therapy in nuclear medicine. Tb-155 is of interest for SPECT imaging and/or Auger therapy. High radionuclide purity is mandatory for many applications in medicine. The quantification of the activity of the produced contaminants is therefore as important as that of the radionuclide of interest. The experiments performed at the ARRONAX cyclotron (Nantes, France), using the deuteron beam delivered up to 34 MeV, provide an additional measurement of the excitation function of the Gd-nat(d,x)Tb-155 reaction and of the produced terbium and gadolinium contaminants. In this study, we investigate the achievable yield for each radionuclide produced in natural gadolinium as a function of the deuteron energy. Other reactions are discussed in order to define the production route that could provide Tb-155 with a high yield and a high radionuclide purity. This article aims to improve data for the Gd-nat(d,x) reaction and to optimize the irradiation conditions required to produce Tb-155.

1. Introduction

Auger electrons have a great potential for therapy thanks to their high linear energy transfer on a very short range in matter. The use of Auger electrons to destroy cells has been proposed in 1975 (Feinendegen, 1975). Feinendegen described the biological effects of Auger electrons: cell death, DNA break, mutation. The effects are localized around the site where the Auger electron is emitted. Indeed, Auger electrons have an energy from few keV to several tens of keV, depending on the element, corresponding to a stopping power in tissue from 1000 keV/μm to 50 keV/μm and a range in water between few nanometers and several micrometers. Tb-155 is an Auger electron and a conversion electron emitter. Tb-155 emits gamma rays suited for the Single Photon Emission Computed Tomography (SPECT). In 2012, results have been published (Müller et al., 2012) on the good tumor visualization using Tb-155 in SPECT, as well as with Tb-152 in PET.

Recently, there is a growing interest in the terbium element for medical applications. It has been called the “Swiss knife” of nuclear medicine (Müller et al., 2012) because Tb-152 is of interest for Positron Emission Tomography (PET), Tb-155 for Single Photon Emission Computed Tomography (SPECT), Tb-149 and Tb-161 can respectively be used for alpha and beta- radionuclide targeted therapy. The therapeutic effectiveness of Tb-149 and Tb-161 has been shown (Müller et al., 2012) and a study has concluded that terbium isotopes are suited for both therapy and diagnosis (Chopra, 2012).

Nowadays, Tb-155 is available using 1.4 GeV protons on a tantalum target followed by a mass separation process at ISOLDE (CERN) that allows to start medical researches. However, this type of facility is too complex and too expensive, in comparison with conventional radionuclide production methods, to be used for industrial development. Direct production routes have to be investigated using low energy particles.

In this work, Tb-155 has been selected in the frame of the production study of Auger electron emitters with the ARRONAX cyclotron.

With natural gadolinium targets, the production of Tb-155 is possible using proton, deuteron or α particle as projectile. We focused our study on new production cross section data measurements using deuteron as projectile. Our data are compared with the experimental results of Tárkányi et al. published in 2014, those of Szelecsényi et al. published in 2016, and with the values of the TALYS 1.6 code. The production yield of each radionuclide formed in the Gd-nat target has been calculated. The radionuclide purity is discussed and compared with other production routes, in order to determine the most appropriates one for Tb-155 production.

Moreover, our new data and nuclear data in general, are of interest to improve the databases and the theoretical models. They are also useful for material activation calculations and for some industries. We

* Corresponding author.
E-mail address: Charlotte.Duchemin@subatech.in2p3.fr (C. Duchemin).

http://dx.doi.org/10.1016/j.apradiso.2016.09.030
Received 21 April 2016; Received in revised form 27 September 2016; Accepted 28 September 2016
Available online 30 September 2016

Table 1
isotopic composition of the gadolinium foils provided by the Good Fellow company.

Gd-152	Gd-154	Gd-155	Gd-156	Gd-157	Gd-158	Gd-160
0.2%	2.2%	14.8%	20.5%	15.7%	24.8%	21.8%

can cite, in particular, the local activation method that finds application in the automotive sector for the measurement of nanometric to micrometric wear and corrosion (Conlon, 1974; IAEA, 1997).

2. Materials and methods

2.1. Experimental set-up

The cross section measurements are performed at the ARRONAX cyclotron using the stacked-foil method (Blessing et al., 1995; Duchemin et al., 2015), which consists in the irradiation of a set of thin foils, grouped as patterns. Each pattern contains a target to produce the investigated radionuclide, a monitor foil to have information on the beam flux through a reference reaction recommended by the International Atomic Energy Agency and a degrader foil to change the incident beam energy for the irradiation of the next pattern with a lower energy. In this work, terbium and gadolinium isotopes are produced in natural abundance gadolinium foils, provided by the GoodFellow company (see GoodFellow website), with a chemical purity of 99%. The isotopic composition of the Gd-nat target is reported in Table 1.

Each foil has been weighed before irradiation using an accurate scale ($\pm 10^{-5}$ g) and scanned to precisely determine its area. From these values and assuming that the foil is homogeneous over the whole surface, the thickness is deduced. 25 μm thick gadolinium target foils, 10 μm titanium monitor foils with 99.6% chemical purity were used in this work. 100, 500 and 900 μm thick aluminium degrader foils were used to change the energy beam through the stacks.

The ARRONAX cyclotron delivers deuteron beams up to 34 MeV (Haddad et al., 2008). The deuteron beam energy uncertainty is ± 0.25 MeV, as determined from simulations by the cyclotron provider. The beam line is closed using a 75 μm thick kapton foil that makes a barrier between the air in the vault and the vacuum in the line. The stacks were located about 7 cm downstream in air. The energy through each thin foil was determined in the middle of the thickness of the foil using the SRIM software (Ziegler et al., 2010). Energy losses in the kapton foil and in the air were taken into account. All along the stack, depending on the number of foils, the energy uncertainty calculated using the SRIM software increases up to 0.9 MeV due to spatial and energy straggling and the initial energy beam spread. Several stacks were irradiated with different incident energies in order to minimize the energy spread and to cover the energy range from 33.3 MeV down to 10.5 MeV (see Table 2). A typical irradiation was carried out with a mean beam intensity of 110 nA during 30 min.

For each irradiation, an instrumented beam stop was used to control the beam current stability. However, it was not used as a Faraday cup since it is not equipped with an electron suppression device.

For all the experiments, the recommended cross section values of the Ti-nat(d,x)V-48 reaction (Tárkányi et al., 2001) were used to measure the particle flux. There is a drawback in using a relative calculation, regarding the possible change in the recommended values when new more accurate measurements are available. The same problem exists for decay constants, γ emission branching ratios, etc, used to calculate the cross sections. Being aware of this problem, we decided to mention the mean energy crossed by each monitor foil, for which our data have been obtained (see Table 3). If the recommended values change (Tárkányi et al., 2014) in the coming years, the cross section data can be modified accordingly.

The activity measurements in each foil were performed using a high purity germanium detector from Canberra (France) with low background lead and copper shielding, checked by a quality control once a week. Gamma spectra were recorded in a suitable geometry calibrated in energy and efficiency with standard Co-57,60 and Eu-152 gamma sources from LEA-CERCA (France). The full widths at half maximum were 1.04 keV at 122 keV (Co-57 γ ray) and 1.97 keV at 1332 keV (Co-60 γ ray). The samples were placed at a height of 19 cm from the detector in order to reduce the dead time and the occurrence of sum peaks. The dead time during the counting was always kept below 10%.

2.2. Data processing

All the activity values of the radionuclides produced in the foils were calculated from the γ spectra and the nuclear decay data (QCALC, 1995; Kinsey, 1996; Ekström and Firestone, 2004) given in Table 5. The spectra were analyzed, using the Fitzpeaks spectroscopy software (FitzPeaks Gamma Analysis and Calibration Software version 3.66). The first activity measurements were performed, for each foil, for one hour the day after the irradiation with a cooling time of about 14 h. The second ones were performed later, with a counting time from a minimum of 24 h and up to 60 h. The gadolinium targets have been measured a third time one month and a half after the EOB, in order to reduce the uncertainty on the activity of Tb-160 and Gd-153. In addition, these measurements have permitted to get the cumulative activity of Gd-153, obtained after the complete decay of Tb-153, and to confirm the Tb-155 activity values obtained with the two other measurements. It has also led to the measurement of the cumulative activity of Tb-156 g(m1+,m2+). The monitor foils have been measured three weeks after the end of beam (EOB), waiting for the complete decay of scandium-48. Indeed, Sc-48 ($T_{1/2}$=43.67 (9) h) has common gamma lines with the radionuclide of reference, vanadium-48 ($T_{1/2}$=15.9735 (25) days). Nuclear data associated to V-48 are summarized in Table 4.

Knowing the precise thickness of the foil and the total activity of the isotopes formed in the target, their production cross sections are calculated using the activation formula (1) with the appropriate projectile flux.

$$\sigma(E) = \frac{Act(E)\cdot A}{\chi\cdot\phi\cdot N_a\cdot M\cdot(1 - e^{-\lambda t})} \quad (1)$$

In Eq. (1), the production cross section *σ(E)* (mb) of a radionuclide depends on its activity corrected to the EOB - *Act(E)* (Bq). The activity is deduced from a recorded gamma spectrum and the net peak area of the associated radionuclide gamma emission, from the detector efficiency, from the live time and real time of the measurement, the gamma emission probability and the radionuclide half-life. Moreover,

Table 2
Energy values in the middle of the gadolinium target foils.

Deuteron energy (MeV)	Mean beam intensity (nA)	Foil 1	Foil 2	Foil 3	Foil 4	Foil 5
		Gd	Gd	Gd	Gd	Gd
34.00 (25)	118	33.34 (30)	29.91 (42)	26.09 (52)	21.82 (64)	
28.70 (25)	108	27.95 (29)	24.56 (40)	16.16 (65)	14.43 (73)	10.55 (93)
24.00 (25)	105	23.13 (29)	18.36 (46)	12.36 (66)		

Table 3
energy values in the middle of the titanium monitor foils.

Deuteron energy (MeV)	Mean beam intensity (nA)	Foil 1	Foil 2	Foil 3	Foil 4	Foil 5
		Ti	Ti	Ti	Ti	Ti
34.00 (25)	118	33.15 (30)	29.70 (43)	25.87 (54)	21.56 (66)	
28.70 (25)	108	27.74 (33)	24.35 (46)	15.89 (69)	14.09 (74)	10.18 (95)
24.00 (25)	105	22.88 (33)	18.07 (46)	11.99 (67)		

Table 4
vanadium-48 half-life and main γ rays (Kinsey, 1996).

Radionuclide	$T_{1/2}$ (days)	E_γ (keV)	I_γ (%)
V-48	15.9735 (25)	944.130	7.870 (7)
		983.525	99.98 (4)
		1312.106	98.2 (3)

for a given target material, the activation formula depends on its decay constant λ (s^{-1}) and its atomic mass A (g mol^{-1}). It also depends on the target areal density M (g cm^{-2}), its chemical purity and/or isotopic abundance χ (only the chemical purity in the case of a natural target), the Avogadro constant (N_a), the irradiation duration t (s) and the projectile flux ϕ (particle s^{-1}). This last parameter is usually obtained from the beam current measurement.

In our experiment, each target thin foil received the same flux as the monitor foil placed behind it. The beam energy impinging each foils is slightly different, with E for the target and E′ for the monitor. It is possible to define a relative Eq. (2), in which the knowledge of the beam current is no longer necessary. In this equation, the prime parameters are associated to the production of V-48 in the titanium foils, used as isotope of reference with a recommended cross section. The other ones relate to the radionuclide produced in the gadolinium target.

$$\sigma(E) = \sigma'(E')\cdot\frac{\chi'\cdot Act(E)\cdot A\cdot M'\cdot(1-e^{-\lambda' t})}{\chi\cdot Act'(E')\cdot A'\cdot M\cdot(1-e^{-\lambda t})} \quad (2)$$

The cross section uncertainty is estimated with a propagation error calculation. Since all the parameters of Eq. (2) are independent, the total error is expressed as a quadratic sum (see Eq. (3)).

$$\frac{\Delta\sigma(E)}{\sigma(E)} = \sqrt{\left(\frac{\Delta\sigma'(E')}{\sigma'(E')}\right)^2 + \left(\frac{\Delta Act(E)}{Act(E)}\right)^2 + \left(\frac{\Delta Act'(E')}{Act'(E')}\right)^2 + \left(\frac{\Delta M}{M}\right)^2 + \left(\frac{\Delta M'}{M'}\right)^2} \quad (3)$$

The main error sources come from the recommended cross section values, the activity values of each produced radionuclide and the foil thickness. Since no uncertainty is given for the recommended cross section values, we have decided to use the uncertainty of the nearest experimental value used by the IAEA to perform the adjustment. It leads to an uncertainty of 11.4% in average. The uncertainty on the activity of a radionuclide produced in the gadolinium targets depends on different parameters such as the uncertainty on the gamma line branching ratio, the radionuclide half-life (see Table 5), the detector efficiency, the dead time. These uncertainties are, in average, of 3.4% for the Tb-155 activity and 2.9% for the V-48 activity. Around 1% of uncertainty is calculated for the areal density. The contribution of the uncertainty on the irradiation time is not significant and has been neglected.

2.3. The comparison with the TALYS 1.6 code

In this work, all the experimental cross section values are compared with the TALYS code version 1.6 released in December 2013 (Koning and Rochman, 2012). TALYS is a nuclear reaction program to simulate reaction induced by light particles on nuclei heavier than carbon. It incorporates theoretical models to predict observables including theoretical cross section values as a function of the incident particle energy (from 1 keV to 1 GeV). A combination of models that better describes the whole set of available data for all projectiles, targets and incident energies have been defined by the authors and put as default in the code. In this way, a calculation can be performed with minimum information in the input file: the type of projectile and its incident energy, the target type and its mass. The results are plotted as TALYS 1.6 default in Fig. 1. Since there are some differences between experimental data and the results of the TALYS code using default models, we have performed the calculations using a combination of models (models already included in the TALYS code) that better describes the production cross sections, for a variety of projectiles, incident energies and target masses.

The description of the optical, preequilibrium and level density models has been found to have a great influence on the calculated production cross section values. Better results are, in general, obtained (Duchemin, 2015) for deuterons used as projectile with the optical model described by Han et al. (Han et al., 2006), a preequilibrium model based on the exciton model including numerical transition rates with optical model for collision probability (Gadioli and Hodgson, 1992) and a model for the microscopic level density from Hilaire's combinatorial tables (Goriely et al., 2008). The results of this combination of models are referenced in the following figures as TALYS 1.6 Adj. It has to be noticed that the same previously cited models for preequilibrium emission and level density give better agreement for proton and alpha particle as projectile.

3. Results

3.1. The Tb-155 production cross section

Tb-155 has a half-life of 5.32 (6) days. It decays by Electron Capture (EC) process to Gd-155 (stable) by emitting Auger electrons (4.84 keV and 34.9 keV), conversion electrons (from 2 keV to 130 keV) and nine main gamma rays (from 86 keV to 367 keV). The gamma lines used to determine the Tb-155 activity in the γ spectra are listed in Table 5.

Our experimental production cross section points are plotted as full circle in Fig. 1, compared with the work of Tárkányi et al. (2014) and Szelecsényi et al. (2016), and with the results of the TALYS 1.6 code.

Our experimental values, obtained in the energy range from 10.5 to 33.3 MeV, show different bumps in agreement with the reaction routes leading to the Tb-155 production: Gd-155(d,2 n) with $E_{threshold}$=3.88 MeV, Gd-156(d,3 n) ($E_{threshold}$=12.52 MeV) and Gd-157(d,4 n) ($E_{threshold}$=18.96 MeV). Our new excitation function shows a maximum around 320 mb at 25 MeV. Our data are in agreement with those published by Tárkányi et al. in 2014 up to 18 MeV. From 18 to 25 MeV, the literature data show some fluctuations. Above 25 MeV, our values are lower than those of Tárkányi et al. but still agree with each other within their error bars. The values of Szelecsényi et al. (2016), measured from 4 to 21 MeV, show the same trend as our points with higher values but also in agreement within their error bars. The TALYS code results using default models give a

Table 5
Produced terbium and gadolinium radionuclides physical characteristics and Q-value (QCALC, 1995, Kinsey, 1996; Ekström and Firestone, 2004). *Tb-154m1 and Tb-154m2 Q values have been obtained from the TALYS code.*

Radionuclide	$T_{1/2}$	E_γ (keV)	I_γ (%)	Contributing reactions	Q value (MeV)
Tb-151	17.609 (1) h	108.088	24.3 (9)	Gd-152(d,3n)	−14.16
		251.863	26.3 (9)	Gd-154(d,5n)	−29.30
Tb-152	17.5 (1) h	344.2785	65	Gd-152(d,2n)	−7.00
				Gd-154(d,4n)	−22.14
				Gd-155(d,5n)	−28.57
Tb-153	2.34 (1) d	102.2564	6.4 (4)	Gd-152(d,n)	1.67
		109.7601	6.76 (25)	Gd-154(d,3n)	−13.47
		141.914	1.073 (19)	Gd-155(d,4n)	−19.91
		170.4511	6.3 (3)	Gd-156(d,5n)	−28.44
		210.1945	1.36 (12)		
		212.004	31.0 (16)		
		249.546	2.33 (6)		
		835.48	1.04 (3)		
Tb-154g	21.5 (4) h	704.9	4.8 (3)	Gd-154(d,2n)	−6.56
		1291.326	6.9 (4)	Gd-155(d,3n)	−12.99
		1324.9	1.17 (9)	Gd-156(d,4n)	−21.53
		1414.49	1.92 (15)	Gd-157(d,5n)	−27.89
Tb-154m1	9.4 (4) h	415.85	2.11 (14)	Gd-154(d,2n)	−6.66
		540.18	20	Gd-155(d,3n)	−13.09
		1152.42	2.2 (3)	Gd-156(d,4n)	−21.63
		1288.39	1.39 (12)	Gd-157(d,5n)	−27.99
		1965.03	1.94 (14)		
Tb-154m2	22.7 (5) h	171.99	4.6 (4)	Gd-154(d,2n)	−6.76
		225.94	26.8 (21)	Gd-155(d,3n)	−13.19
		265.83	3.9 (4)	Gd-156(d,4n)	−21.73
		267.5	3.9 (4)	Gd-157(d,5n)	−28.09
		304.75	1.42 (4)		
		426.78	17		
		479.18	3.8 (4)		
		565.33	2.59 (24)		
		888.8	1.40 (21)		
		992.92	16.2 (14)		
Tb-155	5.32 (6) d	148.65	2.648 (23)	Gd-154(d,n)	2.61
		180.103	7.45 (15)	Gd-155(d,2n)	−3.83
		340.69	1.182 (23)	Gd-156(d,3n)	−12.36
				Gd-157(d,4n)	−18.72
				Gd-158(d,5n)	−26.66
Tb-156g	5.35 (6) d	199.2132	40.9 (2.2)	Gd-155(d,n)	3.09
		262.579	5.8 (3)	Gd-156(d,2n)	−5.45
		296.526	4.46 (3)	Gd-157(d,3n)	−11.81
		356.426	13.61 (7)	Gd-158(d,4n)	−19.75
		422.38	7.95 (4)		
		534.318	66.6 (3)		
		780.23	2.347 (15)		
		926.26	3.41 (3)		
		949.08	1.609 (15)		
		959.86	1.962 (19)		
		1037.76	1.045 (12)		
		1065.15	10.77 (5)		
		1067.19	2.812 (25)		
		1154.19	10.37 (5)		
		1159.04	7.25 (3)		
		1222.36	31.00 (12)		
		1266.36	1.073 (12)		
		1334.46	2.539 (19)		
		1421.44	12.23 (5)		
Tb-160	72.3 (2) d	197.0352	5.18 (3)	Gd-160(d,2n)	−3.11
		215.646	4.018 (15)		
		298.58	26.13 (18)		
		392.514	1.336 (9)		
		765.28	2.140 (12)		
		879.383	30.10 (6)		
		962.317	9.81 (9)		
		966.171	25.10 (12)		
		1002.88	1.038 (6)		
		1115.12	1.565 (15)		
		1177.962	14.87 (6)		
		1199.89	2.384 (12)		
		1271.88	7.444 (21)		
Gd-153	240.4 (10) d	97.431	29	Gd-152(d,p)	4.02
		103.18	21.11 (23)	Gd-154(d,2n+p)	−11.12

(continued on next page)

Table 5 *(continued)*

Radionuclide	$T_{1/2}$	E_γ (keV)	I_γ (%)	Contributing reactions	Q value (MeV)
				Gd-155(d,3n+p)	−17.55
				Gd-156(d,4n+p)	−26.09
				Gd-157(d,5n+p)	−32.45
Gd-159	18.479 (4) h	363.55	11.4 (6)	Gd-158(d,p)	3.72
				Gd-160(d,2n+p)	−9.68

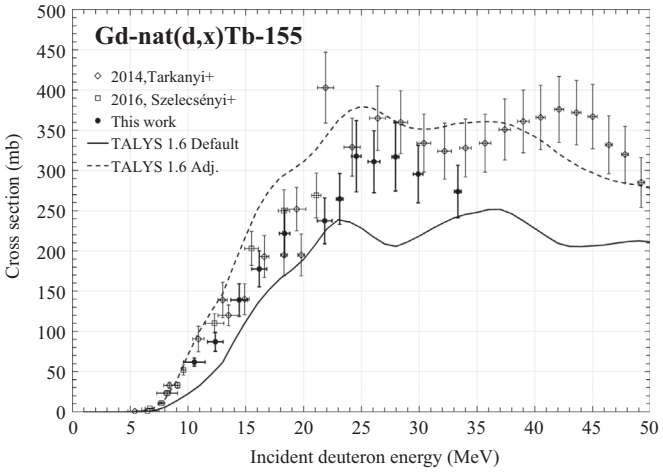

Fig. 1. experimental cross section of Gd-nat(d,x)Tb-155.

first maximum at 23 MeV, in disagreement with the experimental one, which is close to 25 MeV. With TALYS 1.6 Adj. this maximum is well reproduced at 25 MeV. However, the amplitudes of the cross section given by both combination of models differ from the experimental ones.

3.2. The Tb-155 contaminants production cross sections

New production cross section values have been determined for Tb-151, Tb-152, Tb-153, Tb-154 m, Tb-156 g, Tb-160, Gd-153 and Gd-159 also produced in the natural gadolinium target during the irradiations. Their physical characteristics are listed in Table 5 and the production cross sections values are presented in Table 6 and in Figs. 2-10. Our new production cross section results are, in general, in good agreement with the values published by Tárkányi et al. (2014), and Szelecsényi et al. (2016). The TALYS code shows some disagreements excepted for Tb-153, Tb-156g and Tb-160, for which the TALYS 1.6 Adj values give an overall good agreement with the experimental points.

3.3. The Tb-155 and contaminants thick target production yields (TTY)

Using the cross section values as a function of the energy σ(E) obtained either in this work or in databases, we have calculated the associated Thick Target production Yields in MBq for one hour of irradiation and 1 μAe, also called 1 h-1 μA yield. The values are obtained as a function of the projectile energy, using the following expression:

$$TTY = \phi.\chi.\frac{N_{a.\rho}}{A}(1 - e^{-\lambda.t})\int_{Emin}^{Emax}\frac{\sigma(E)}{\frac{dE}{dx}}dE \quad (4)$$

In relation (4), ϕ is the number of particles per second delivered in

Table 6
Production cross section values from the Gd-nat(d,x) reaction.

Energy (MeV)	σ Tb-151 (mb)	σ Tb-152 (mb)	σ Tb-153 (mb)	σ Tb-154m1 (ind.) (mb)	σ Tb-154m2 (ind.) (mb)
33.34 ± 0.30		14.45 ± 1.76	150.07 ± 18.72	247.59 ± 42.10	21.28 ± 2.96
29.91 ± 0.42	1.74 ± 0.45	6.85 ± 0.88	113.16 ± 14.78	216.18 ± 36.56	18.49 ± 2.59
27.95 ± 0.30	1.89 ± 0.56	5.08 ± 0.68	108.23 ± 13.64	223.77 ± 33.49	18.89 ± 2.54
26.09 ± 0.52	1.84 ± 0.53	0.79 ± 0.28	48.95 ± 6.43	170.12 ± 28.71	14.25 ± 2.17
24.56 ± 0.40	2.13 ± 0.54		47.64 ± 6.13	187.55 ± 26.69	15.07 ± 2.15
23.13 ± 0.29	1.66 ± 0.39	0.67 ± 0.21	23.38 ± 3.15	161.63 ± 25.95	11.89 ± 1.70
21.82 ± 0.64	1.03 ± 0.33	0.99 ± 0.22	18.53 ± 2.56	140.99 ± 23.15	9.67 ± 1.47
18.36 ± 0.46		1.85 ± 0.32	7.92 ± 1.18	92.24 ± 15.74	5.63 ± 0.99
16.16 ± 0.65		1.79 ± 0.29	3.75 ± 0.56	57.13 ± 8.11	3.45 ± 0.66
14.43 ± 0.73		1.65 ± 0.24	0.80 ± 0.15	25.18 ± 3.65	1.49 ± 0.35
12.36 ± 0.66				9.28 ± 1.78	0.74 ± 0.27
10.55 ± 0.93		0.61 ± 0.06	0.32 ± 0.08	6.38 ± 0.95	0.60 ± 0.21
Energy (MeV)	σ Tb-155 (mb)	σ Tb-156g (mb)	σ Tb-160 (mb)	σ Gd-153 (cum.) (mb)	σ Gd-159 (mb)
33.34 ± 0.30	273.90 ± 32.58	318.59 ± 37.62	13.81 ± 1.78	160.96 ± 31.23	70.93 ± 11.67
29.91 ± 0.42	295.61 ± 35.79	304.59 ± 36.94	16.83 ± 2.15	118.67 ± 22.96	67.29 ± 11.11
27.95 ± 0.30	316.92 ± 42.49	297.45 ± 40.80	18.95 ± 2.60	110.41 ± 21.65	69.90 ± 11.28
26.09 ± 0.52	310.90 ± 38.47	259.32 ± 31.83	23.02 ± 3.14	47.95 ± 9.61	54.60 ± 9.30
24.56 ± 0.40	317.67 ± 44.25	249.08 ± 34.69	24.24 ± 3.33	50.78 ± 10.61	59.19 ± 9.70
23.13 ± 0.29	264.73 ± 31.67	234.17 ± 27.60	26.24 ± 3.21	24.92 ± 5.10	45.50 ± 7.52
21.82 ± 0.64	237.45 ± 28.51	226.10 ± 27.06	29.21 ± 3.64	18.00 ± 3.60	42.63 ± 7.10
18.36 ± 0.46	221.67 ± 29.01	264.27 ± 34.34	48.68 ± 6.41	8.18 ± 1.97	48.15 ± 8.39
16.16 ± 0.65	177.61 ± 22.47	213.29 ± 27.79	52.97 ± 6.35	5.07 ± 1.30	47.23 ± 7.67
14.43 ± 0.73	139.04 ± 20.00	187.66 ± 26.02	77.30 ± 9.36		52.90 ± 8.39
12.36 ± 0.66	86.96 ± 11.71	117.44 ± 15.39	127.12 ± 16.66		61.30 ± 10.56
10.55 ± 0.93	61.90 ± 4.98	88.65 ± 6.79	88.85 ± 7.12		46.20 ± 6.16

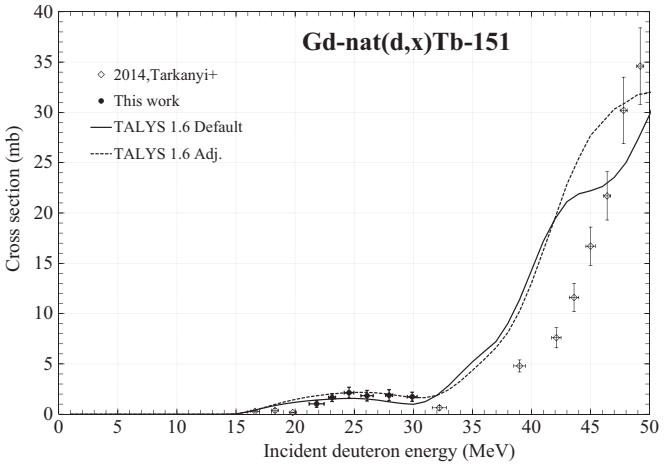

Fig. 2. Experimental cross section of Gd-nat(d,x)Tb-151.

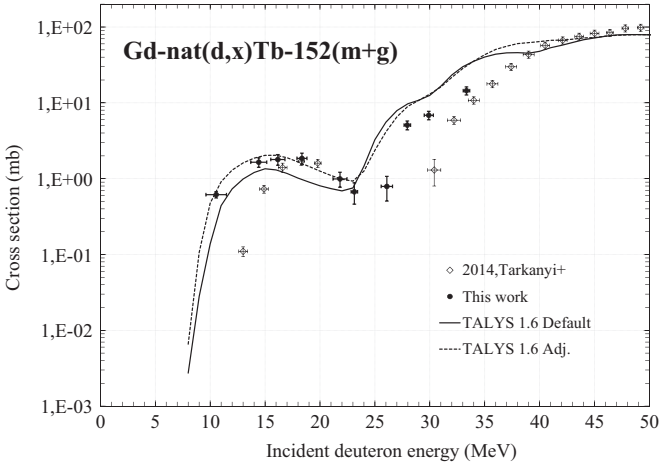

Fig. 3. Experimental cross section of Gd-nat(d,x)Tb-152.

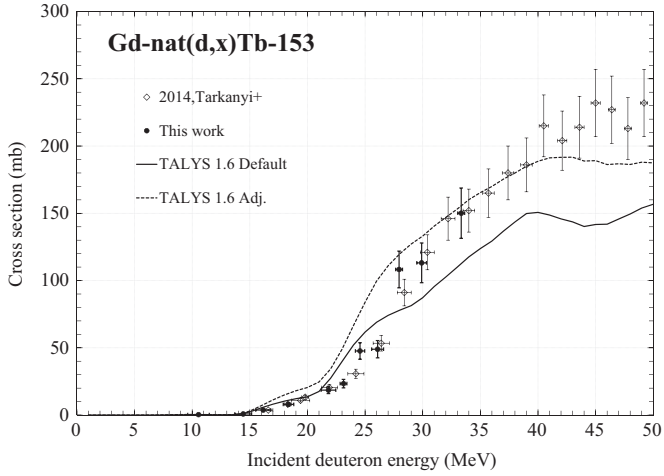

Fig. 4. Experimental cross section of Gd-nat(d,x)Tb-153.

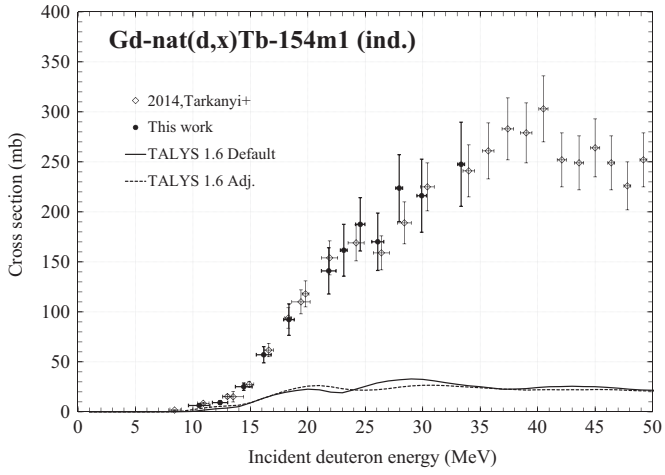

Fig. 5. Experimental cross section of Gd-nat(d,x)Tb-154m1.

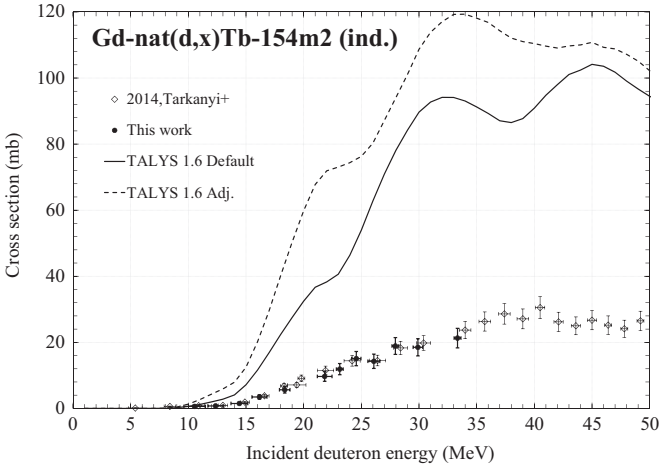

Fig. 6. Experimental cross section of Gd-nat(d,x)Tb-154m2.

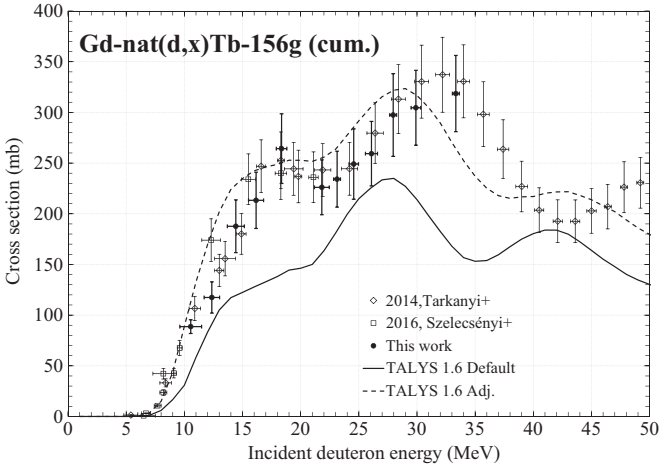

Fig. 7. Experimental cross section of Gd-nat(d,x)Tb-156g.

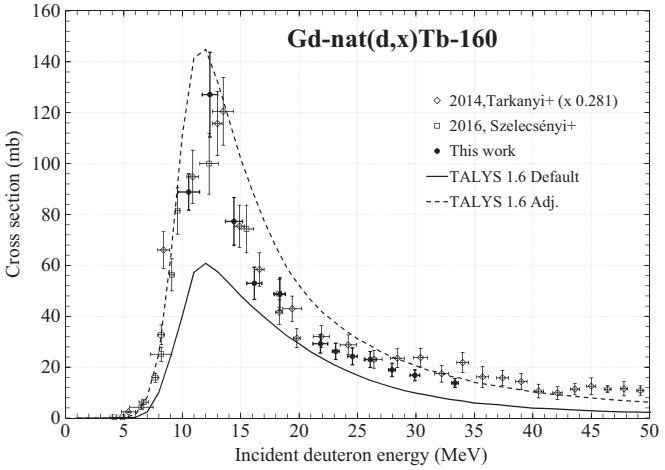

Fig. 8. Experimental cross section of Gd-nat(d,x)Tb-160.

one μAe. The irradiation time, t, is set at one hour. χ corresponds to the chemical purity and/or isotopic abundance of the target (only the chemical purity in the case of a natural target), ρ is the target density (g cm^{-3}) and N_a is the Avogadro constant. $\frac{dE}{dx}$ is the linear energy transfer of the projectile in the target material (MeV cm^{-1}). In a thick target, the incident particle energy decreases with the penetration depth. E_{max} corresponds to the incoming projectile energy, whereas E_{min} corresponds to the outgoing projectile energy.

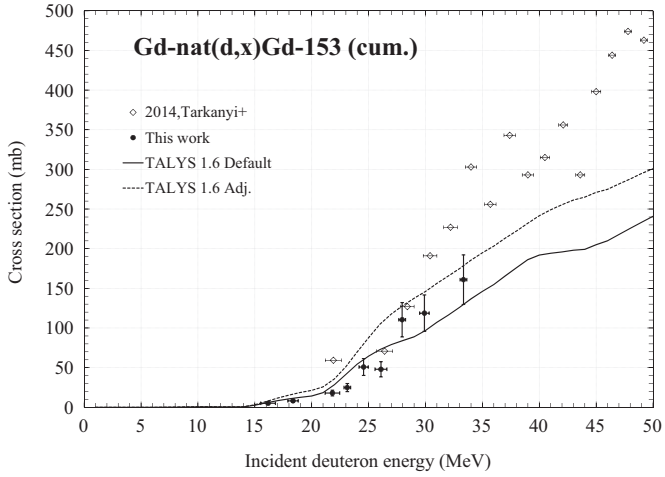

Fig. 9. Experimental cross section of Gd-nat(d,x)Gd-153.

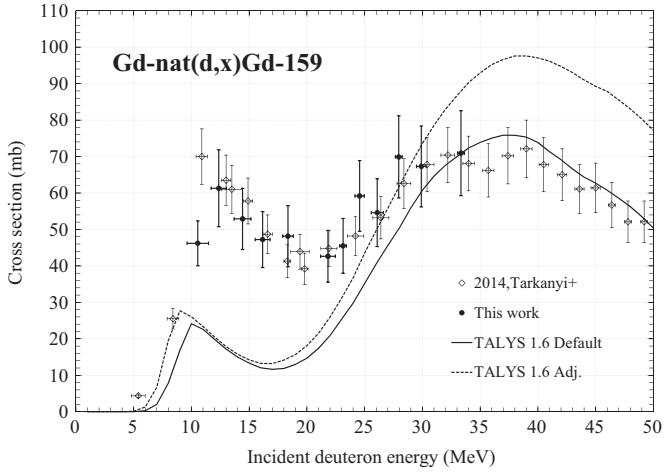

Fig. 10. Experimental cross section of Gd-nat(d,x)Gd-159.

The production yields are presented in Fig. 11 for the Gd and Tb radionuclides measured in this work.

The Tb-155 1 h-1 μA yield (see Fig. 11) reaches 39.9 MBq at 33.3 MeV. This activity could be obtained using a natural gadolinium target of 1.8 mm thick, which allows to produce Tb-155 from 33.3 MeV down to the Gd-155(d,2 n) reaction energy threshold (4.9 MeV).

Two gadolinium isotopes have been detected and quantified from

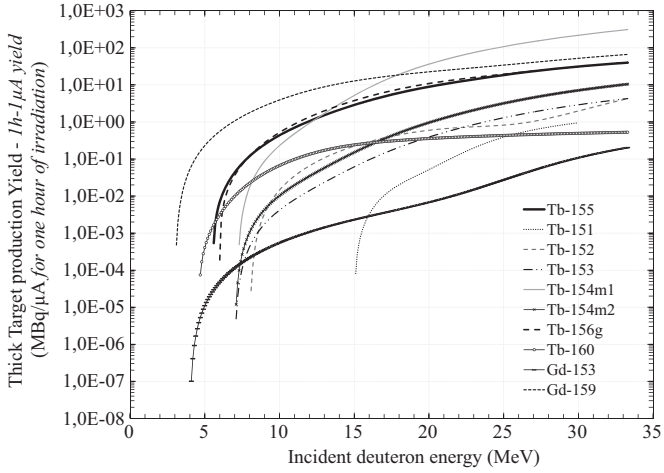

Fig. 11. Production yields calculated for 1 μAe and 1 h of irradiation, from our experimental cross section values obtained for the Gd-nat(d,x) reaction.

our experiments (see Fig. 11). In the frame of Tb-155 production, these elements could be eliminated from the sample by chemical separation.

Tb-151, Tb-152 and Tb-154 have pretty short half-live as compared to Tb-155 and the target can be left for decay or partial decay to reduce their contribution. Tb-153 with a half-life of 2.34 days will remain in part in the final product. It is also the case for Tb-160, with a long half-life of 72.3 days, but produced in lower quantities than Tb-155 (70 times less). Although Tb-157 ($T_{1/2}$=71 (7) y) and Tb-158 ($T_{1/2}$=180 (11) y) have not been measured, their production have to be considered. All these remaining contaminants will decrease the radionuclide purity of the sample.

Moreover, Tb-155 and Tb-156 g (also a decay product of its metastable states Tb-156m1,m2) have close half-live and similar production yield values. In the context of medical applications, the presence of Tb-156 g in the Tb-155 drug will highly increase the dose received by the patient and staff, due to the high energy emissions. Indeed, Tb-156 g emits several γ rays during its decay to Gd-156 (stable), with energies higher than 1.8 MeV and branching ratios higher than 1%.

The production of all the terbium contaminants measured in this work decreases the radionuclide purity from 23.1% at 15 MeV down to 9.7% at 33.3 MeV.

With Gd-nat, the Tb-155 production could be assessed with the purity required for medical applications only using a mass separation device (Augusto et al., 2014) to avoid all the contaminants previously discussed. However, this is not yet available at an industrial level due to financial reasons.

3.4. The comparison between different Tb-155 production routes using Gd-nat as target material

The Fig. 12 shows Tb-155 1 h-1 μA yield values as a function of the incident particle energy calculated from production cross section values published for Gd-nat(α,x) (Gayoso et al., 1996), Gd-nat(p,x) (Vermeulen et al., 2012) and Gd-nat(d,x) (Tárkányi et al., 2014; Szelecsényi et al., 2016) reactions. These values are compared with the ones obtained from our cross section measurements with deuterons (This work).

In the case of deuteron as projectile, the production yield obtained from our data has a similar behavior than that obtained with the values published by Tárkányi et al. (2014) and Szelecsényi et al. (2016) but are lower (up to 16%). The observation of a same trend with lower values has been already highlighted with the cross section values (results shown in part. Section 3.1). With 30 MeV protons as projectiles, the production yield calculated from Vermeulen et al. experimental cross section values (Vermeulen et al., 2012) is 29% higher in comparison with the results of this work using 30 MeV deuterons. At 50 MeV, the use of proton or deuteron as projectile leads to close production yield values. Finally, the results plotted in Fig. 12 show that the lowest production yield values are obtained for α particles as projectiles on Gd-nat. In addition, the number of accelerators able to deliver high energy α particles (higher than 50 MeV) are limited. This last production route seems not suited for Tb-155 routine production.

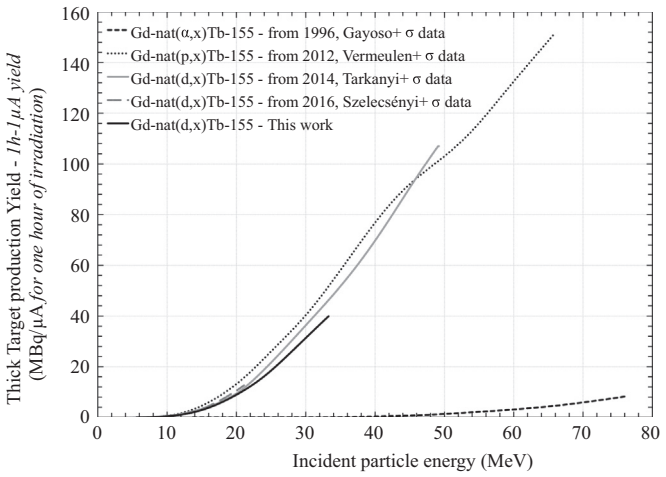

Fig. 12. Tb-155 production yield comparison between proton, deuteron and α particle as projectile on Gd-nat.

The highest activities are obtained with proton as projectile up to 45 MeV but the values are close to those calculated with deuteron as projectile. In this later case, the main advantage is related to the lower amount of target material required to produce the same amount of activity. However, the main drawback is associated to the limited number of accelerators delivering high energy deuteron beams.

The choice of the isotopic composition of the target and of appropriate irradiation conditions have to be set to produce high activities of Tb-155 and to avoid/limit the presence of terbium contaminants, in order to get a high specific activity of the final product. Based on studies with protons or deuterons, we have identified Gd-155 and Gd-154, respectively, as two target isotopes allowing to limit the production of contaminants. These two isotopes have the advantage to avoid the production of the Tb-156g(m1+,m2+) and of the long half-live Tb-157, Tb-158 and Tb-160 radionuclides. Another possibility is to produce Tb-155 indirectly through Dy-155 decay.

In the last part of this article, we discuss these different production routes based on commercially available enriched Gd material and we compare them to the Tb-159(p, xn) indirect production route (Steyn et al., 2014; Engle et al., 2015).

3.5. The direct Tb-155 production with enriched Gd

3.5.1. The use of Gd-154 enriched target and deuterons

Tb-155 is produced by the Gd-154(d,n) reaction without energy threshold and Tb-154 is produced above 6.6 MeV by the Gd-154(d,2n) reaction. Although Tb-156 can be produced on Gd-154 from the Gd-154(d,γ) reaction, the associated production cross section is really low. Tb-155 can be produced without contaminants using deuterons below 6.6 MeV. An experimental study of the Tb-154 production from the Gd-154(d,2n) reaction is necessary to know if the Tb-155 production energy range can be enlarged. Unfortunately, Gd-154 atoms are in Gd-nat in a proportion of only 2.2% (see Table 1) leading to an expensive enriched target material. The Trace Sciences International Corporation (Trace Sciences, 2016) company provides Gd-154 in an oxide form with an enrichment rate between 64% and 67%. All these preliminary information lead to the conclusion that Tb-155 could not be produced in large scale from the Gd-154(d,n) reaction with the purity required for medical applications and with a reasonable cost.

3.5.2. The use of Gd-155 enriched target and protons

The Trace Sciences International Corporation company offers Gd-155 in an oxide or chloride form with an enrichment between 90% and 94%, which is much higher than that of Gd-154 previously discussed. In addition, the material cost will be lower than for Gd-154 as Gd-155 represents 14.8% of the atoms in natural gadolinium. Tb-155 can be produced using protons and Gd-155 through the Gd-155(p,n) reaction (the energy threshold is 1.6 MeV). The production of Tb-156 from the Gd-155(p,γ) reaction is negligible (small cross section). Above 10.8 MeV, the Gd-155(p,2n) reaction takes place, producing Tb-154. Tb-155 can then be produced with a limited amount of contaminants using a Gd-155 target and protons with incident energies below 10.8 MeV. This energy is adapted to cyclotrons currently producing fluorine-18. An experimental production cross section study is necessary to determine the amount of Tb-154 than will be produced if an energy higher than 10.8 MeV is used, and then defined an acceptable

limit. An article published in 2012 by Vermeulen et al. shows model calculations, which estimate the Tb-155 production rate from the Gd-155(p,n) reaction. With 11 MeV protons, Tb-155 could be produced with a high radionuclide purity and a production yield of 5.6 MBq/μAh. From this article (Vermeulen et al., 2012) and based on the Gd-155 enrichment rate and activities that could be assessed, the Gd-155(p,n) reaction is economically viable for large scale Tb-155 production from gadolinium.

3.6. The indirect Tb-155 production with Tb-159

Tb-155 can be directly and indirectly obtained from Tb-159(p,x) reactions (Steyn et al., 2014; Engle et al., 2015). Steyn et al. (2014), suggests the use of Tb-159 targets and high energy protons (higher than 50 MeV) to produce Tb-155 for medical applications. In this case, the reaction Tb-159(p,5n) produces dysprosium-155 ($T_{1/2}$=9.9 (2) hours) that entirely decays to Tb-155. Accelerators such as the ARRONAX cyclotron are now available to allow such reaction for commercial production. Two chemical separations are needed: a first one to separate Dy from the target and a second one for the separation of Tb-155 from the Dy isotopes. The experimental results presented in Steyn et al. study show that this production route can led to Tb-155 yields between 40 GBq (1Ci) and 116 GBq (3Ci), based on realistic irradiation conditions (proton energy range from 50 MeV to 70 MeV). However, Dy-157 ($T_{1/2}$=8.14 (4) h) will be co-produced and it decays to Tb-157 with a long half-life of 71 (7) y. Steyn et al. (2014) study shows that a high radionuclide purity can be assessed for Tb-155 production: 99.9% with 60 MeV protons beam and 88% with 70 MeV. This production route has the economic advantage to use natural Tb as target but requires accelerators that deliver high energy proton beams.

4. Conclusion

Terbium is an element of great interest for nuclear medicine. Tb-149 and Tb-161 have shown their therapeutic efficacy. Tb-152 and Tb-155 have permitted tumor visualization using PET and SPECT, respectively. In the frame of our study, Tb-155 has been selected as a potential Auger emitter for therapy thanks to the Auger electrons emitted during its decay to Gd-155. In order to obtain information on the achievable Tb-155 yield with the Gd-nat(d,x) production route, production cross section measurements have been performed at the ARRONAX cyclotron. Our new data are in agreement with the ones published in 2014 by Tárkányi et al. and in 2016 by Szelecsényi et al. Thick Target production Yields have been calculated from our data and compared with the proton and alpha particle induced productions using cross section data available in the literature. Both protons and deuterons show close production rate values. The Gd-nat(α,x) reaction gives the lower production yield values and is not suited for large scale Tb-155 production. The use of Gd-nat leads to the production of contaminants and specially of a huge amount of Tb-156g that has the same half-life as Tb-155. In order to limit the contaminants several options are possible: one is to keep a Gd-nat target and to add a mass separation step to get pure Tb-155. This is not yet technically available at an industrial level for radionuclide production. An alternative is to use enriched material. Gd-154 and Gd-155 target can be used. Gd-155 irradiated by low energy protons seems the most appropriate choice for Tb-155 production. Finally, with the commercial availability of high energy and high intensity cyclotron, the indirect production through Tb-149(p,5n)Dy-155 must be considered.

Acknowledgments

The ARRONAX cyclotron is a project promoted by the Regional Council of Pays de la Loire financed by local authorities, the French Government and the European Union. This work has been, in part, supported by a grant from the French National Agency for Research called “Investissements d′Avenir”, Equipex Arronax-Plus n^{o} ANR-11-EQPX-0004 and Labex n^{o} ANR-11-EQPX-0018-01.

References

Augusto, R.M., Buehler, L., Lawson, Z., Marzari, S., Stachura, M., Stora, T., CERN-MEDICIS collaboration, 2014. CERN-MEDICIS (Medical Isotopes Collected from ISOLDE): A New Facility. Appl. Sci., vol. 4, pp. 265–281, http://dx.doi.org/10.3390/app4020265

Blessing, G., Bräutigam, W., Böge, H.G., Gad, N., Scholten, B., Qaim, S.M., 1995. Internal irradiation system for excitation function measurement via the stacked-foil technique. Appl. Radiat. Isot. 955, 46–49.

Chopra, A., 2012. [149/152/155/161Tb]-Labeled DOTA-folate conjugated to an albumin-binding entity [149/152/155/161Tb]cm09. Molecular Imaging and Contrast Agent Database (MICAD).

Conlon, T.W., 1974. Thin layer activation by accelerated ions-application to measurement of industrial wear. Wear 29, 69–80.

Duchemin, C., Guertin, A., Haddad, F., Michel, N., Métivier, V., 2015. Cross section measurements of deuteron induced nuclear reactions on natural tungsten up to 34 MeV. Appl. Radiat. Isot. 97, 52–58.

Duchemin, C., 2015. PhD thesis. Étude de voies alternatives pour la production de radionucléides innovants pour les applications médicales. Available on ⟨https://tel.archives-ouvertes.fr/tel-01220522⟩.

Ekström, L.F., Firestone, R.B., 2004. Information extracted from the Table of Radioactive Isotopes, version 2.1.

Engle J.W., Mashnik S.G., Parker L.A., Jackman K.R., Bitteker L.J., Ullmann J.L., Gulley M.S., Pillai C., John K.D., Birnbaum E.R. Nortier F.M., 2015. Nuclear excitation functions from 40 to 200 MeV proton irradiation of terbium. Nuclear Instruments and Methods in Physics Research Section B Beam Interactions with Materials and Atoms, 366. ⟨http://dx.doi.org/10.1016/j.nimb.2015.10.049⟩.

Feinendegen, L.E., 1975. Biological damage from the auger effect, possible benefits. Radiat. Environ. Biophys. 12 (2), 85–99.

FitzPeaks Gamma Analysis and Calibration Software version 3.66, produced by JF Computing Services (UK), based on methods presented in Nucl.Instrum. and Methods (1981) 190, 89–99, describing the program SAMPO80 of the Helsinki University of Technology, Finland.

Gadioli, E., Hodgson, P.E., 1992. Pre-Equilibrium Nuclear Reactions. Oxford Sciences Publications, Clarendon Press, Oxford.

Gayoso, R.E., Sonzogni, A.A., Nassiff, S.J., 1996. (α,pxn) Reactions on Natural Gadolinium. Radiochim. Acta 72, 55–60.

GoodFellow website. Tous les matériaux pour la recherche, lindustrie et la production. www.goodfellow.com

Goriely, S., Hilaire, S., Koning, A.J., 2008. Improved microscopic nuclear level densities within the HFB plus combinatorial method. Phys. Rev. C 78, 064307.

Haddad, F., Ferrer, L., Guertin, A., Carlier, T., Michel, N., Barbet, J., Chatal, J.F., 2008. Arronax a high-energy and high-intensity cyclotron for nuclear medicine. Eur. J. Nucl. Med. Mol. Imaging 35, 1377–1387.

Han, Y., Shi, Y., Shen, Q., 2006. Deuteron global optical model potential for energies up to 200 MeV. Phys. Rev. C. 74, 044615.

IAEA, 1997. The thin layer activation method and its applications in industry, IAEA-TECDOC-924, ISSN 1011–4289.

International Atomic Energy Agency website. Nuclear data service, provided by the nuclear data section. ⟨www-nds.iaea.org⟩.

Kinsey R.R. et al., 1996. In: The NUDAT/PCNUDAT Program for Nuclear Data, paper submitted for publication. In: Proceedings of the 9th International Symposium of Capture Gamma-Ray Spectroscopy and Related Topics. Budapest, Hungary, October Data extracted from the NUDAT database, version 2.6.

Koning, A.J., Rochman, D., 2012. Modern nuclear data evaluation with the TALYS code system. Nucl. Data Sheets 113, 2841.

Müller, C., Zhernosekov, K., Koester, U., Johnston, K., Dorrer, H., Hohn, A., van der Walt, N.T., Turler, A., Schibli, R., 2012. A unique matched quadruplet of terbium radioisotopes for PET and SPECT and for α and β- radionuclide therapy: an in vivo proof-of-concept study with a new receptor-targeted folate derivative. J. Nucl. Med. 53, 1951–1959.

QCALC, 1995. Data produced by the code QCALC, written by Burrows, T.W., National Nuclear Data Center, Brookhaven National Laboratory, and based on the Audi-Wapstra Atomic Mass Tables, G. Audi and A.H. Wapstra, The 1995 Update to the Atomic Mass Evaluation., Nucl. Phys. A, 595, 409.

Steyn, et al., 2014. Cross sections of proton-induced reactions on 152Gd, 155Gd and 159Tb with emphasis on the production of selected Tb radionuclides. Nucl. Instrum. Methods Phys. Res. Sect. B 319, 128–140.

Szelecsényi, F., Kovács, Z., Nagatsu, K., Zhang, M.-R., Suzuki, K., 2016. Investigation of deuteron-induced reactions on natGd up to 30 MeV: possibility of production of medically relevant 155Tb and 161Tb radioisotopes. J. Radioanal. Nucl. Chem. 307, 1877–1881. http://dx.doi.org/10.1007/s10967-015-4528-0.

Tárkányi, F., Takács, S., Ditrói, F., Csikai, J., Hermanne, A., Ignatyuk, A.V., 2014. Activation cross-sections of deuteron induced reactions on natGd up to 50 MeV. Appl. Radiat. Isot. 83, 25–35.

Tárkányi, F., Takács, S., Gul, K., Hermanne, A., Mustafa, M.G., Nortier, M., Oblozinsky, P., Qaim, S.M., Scholten, B., Shubin, Yu.N., Youxiang, Z., 2001. Beam monitor reactions, in Charged Particle Cross Section Database for Medical Radioisotope Production: Diagnostic Radioisotopes and Monitor Reactions; IAEA-TECDOC-1211, pp. 49–152, IAEA, Vienna. Database available on ⟨https://www-nds.iaea.org/medportal/⟩, update may 2013.

Trace Sciences International Corporation. The world's most reliable source of stable isotopes. ⟨http://www.tracesciences.com/gd.htm⟩.
Vermeulen, C., Steyn, G.F., Szelecsényi, F., Kovács, Z., Suzuki, K., Nagatsu, K., Fukumura, T., Hohn, A., van der Walt, T.N., 2012. Cross sections of proton induced reactions on natGd with special emphasis on the production possibilities of 152Tb and 155Tb. Nucl. Instrum. Methods Phys. Sect. B: Beam Interact. Mater. At. 275, 24–32.
Ziegler, J.F., Ziegler, M.D., Biersack, J.P., 2010. SRIM The stopping and range of ions in matter. Nucl. Instrum. Methods Phys. Res. Sect. B 268, 1818–1823.

Further reading

Tárkányi, F., Takács, S., Ditrói, F., Csikai, J., Hermanne, A., Ignatyuk, A.V., 2013. Cross-section measurement of some deuteron induced reactions on 160Gd for possible production of the therapeutic radionuclide 161Tb. Int. J. Radioanal. Nucl. Chem. 298, 1385–1392.